

XMM–Newton observation of 4U 1543-475: the X–ray spectrum of a stellar–mass black–hole at low luminosity

N. La Palombara & S. Mereghetti

Istituto di Astrofisica Spaziale e Fisica Cosmica - Sezione di Milano “G.Occhialini”, CNR, via Bassini 15, I-20133 Milano, Italy

Received / Accepted

Abstract. We report the results of an observation of the galactic black–hole binary 4U 1543-475 performed by XMM–Newton on 2002 August 18, about two months after the start of an outburst detected by RXTE. Despite the relatively low flux of the source, corresponding to a luminosity $L_X \sim 4 \times 10^{34} \text{ erg s}^{-1} \sim 10^{-5} L_{\text{EDD}}$, we could obtain a good quality spectrum thanks to the high throughput of the XMM–Newton EPIC instrument. The spectrum is well fit by a power law with photon index $\Gamma=1.9-2$ without any evidence for iron emission lines or for thermal emission from an accretion disk. We could estimate an upper–limit on the disk bolometric luminosity as a function of the colour temperature: it is always lower than $\sim 10^{33} \text{ erg s}^{-1}$, i.e. less than 10 % of the source total luminosity. Finally, we evaluated that the disk colour temperature must satisfy the condition $kT_{\text{col}} < 0.25 \text{ keV}$ in order to obtain an acceptable value for the disk inner radius.

Key words. accretion, accretion disks – black hole physics – stars: individual: 4U 1543-475, II Lupi – X-rays: binaries

1. Introduction

4U 1543-475 is a recurrent X-ray transient containing a black hole. It was discovered during an outburst in 1971 (Matilsky et al. 1972) and observed in outburst again in 1983 (Kitamoto et al. 1984), in 1992 (Harmon et al. 1992) and in 2002 (Park et al. 2004; Kalemci et al. 2004). In the decade–long quiescence periods the flux is lower than $0.1 \mu\text{Crab}$, while the source brightens by a factor greater than 2×10^7 in outburst (Garcia et al. 2001). In the latest outburst, between June and July 2002, the measured flux reached a peak value of 4.2 Crab in the 2–12 keV energy band, comparable to the peak intensities observed in the three previous outbursts (Tanaka & Lewin 1995). The source light curve along the whole outburst showed the characteristic shape of the ‘classic’ X–ray novae, i.e. a fast rise to the outburst peak followed by an exponential decay, with e –folding decay time of $\simeq 14$ days (Mc Clintock & Remillard 2003). The spectrum was soft and dominated by the emission from the accretion disk: its continuum part was fit with a multi–colour disk blackbody ($kT_{\text{max}} = 1.04 \text{ keV}$) and a power–law (photon index $\Gamma \sim 2.7$).

The optical counterpart of 4U 1543-475, II Lupi, has been classified as spectral type A2V (Chevalier & Ilovaisky 1992). During the X–ray outbursts it brightens by $\simeq 1.8$ mag (van Paradijs & Mc Clintock 1995), but during the quiescent periods it was possible to perform detailed studies. This allowed to derive the orbital period $P_{\text{orb}} = 26.8 \text{ hr}$, the black–hole mass $M_1 = 9.4 \pm 2.0 M_{\odot}$, the secondary star mass

$M_2 = 2.7 \pm 1.0 M_{\odot}$, the source distance $d = 7.5 \pm 1.0 \text{ kpc}$ and the orbit inclination $i = 20.7 \pm 1.0^\circ$ (Orosz et al. 1998; Orosz 2003).

Here we present the results of an XMM–Newton observation obtained after the most recent outburst of 4U 1543-475. The spectrum obtained with the EPIC instrument has an unprecedented statistics for a galactic black–hole at this level of luminosity, allowing for the first time to investigate the spectral details of a black–hole binary approaching the quiescent phase.

2. Observations, data reduction and spectral analysis

4U 1543-475 was observed by XMM–Newton on 2002 August 18, between 12:30 and 20:42 UT. The source was on–axis and the observation lasted about 29.5 ks. The three EPIC cameras (Turner et al. 2001; Strüder et al. 2001) were all active during the observation: the PN, MOS1 and MOS2 instruments were operated in *Small Window*, *Timing Uncompressed* and *Full Frame* mode, respectively. For all of them, the Thin filter 1 was used.

We used the version 5.4.1 of the XMM–Newton Science Analysis System (SAS) to process the event files. After the standard processing pipeline of the data, we looked for possible periods of high background due to soft proton flares with energies less than a few hundred keV. For the two MOS cameras this was done by inspecting the light curves of the events with energy above 10 keV detected in the peripheral CCDs and with pixel patterns from 0 to 4. In this way, we selected only those

Table 1. Best-fit parameters for a power-law model in the case of the PN, MOS2 and PN+MOS2 data.

Instrument	N_H ($\cdot 10^{21} \text{ cm}^{-2}$)	Photon Index	Normalization at 1 keV ($\text{ph keV}^{-1} \text{ cm}^{-2} \text{ s}^{-1}$)	χ^2_ν	d.o.f.	f_X (0.3–10 keV) ^a ($\text{erg cm}^{-2} \text{ s}^{-1}$)
PN	3.6 ± 0.2	1.92 ± 0.04	$(9.9 \pm 0.5) \times 10^{-4}$	1.104	297	$(3.7 \pm 0.2) \times 10^{-12}$
MOS2	4.5 ± 0.3	1.99 ± 0.07	$(11.2 \pm 0.9) \times 10^{-4}$	1.131	146	$(3.7 \pm 0.3) \times 10^{-12}$
PN+MOS2	3.8 ± 0.2	1.94 ± 0.04	$(10.3 \pm 0.3) \times 10^{-4}$	1.069	442	$(3.7 \pm 0.1) \times 10^{-12}$

NOTE - Errors are at 90 % c.l. for a single interesting parameter; ^a Absorbed flux

background events whose high energy is distributed in one or two pixels at most, which presumably are due to low energy protons focused on the focal plane by the telescope mirrors. These light curves showed a large increase of the count-rate (up to a factor of ~ 40) during the last 10 ks of the observation. We decided to use for our analysis of 4U 1543-475 only time intervals with count-rates below 0.7 c s^{-1} for this type of events, yielding an effective observing time of 19.9 ks.

Since the PN camera was operated in *Small Window* mode, no data were taken with the peripheral CCDs. Therefore, the data cleaning was based on the events in the central CCD, with energies above 10 keV and pattern 0¹. Also in this case we observed a large increase of the count-rate in the last part of the observation: we selected time periods with count-rates lower than 0.07 c s^{-1} , thus obtaining an effective exposure time of 13.2 ks².

In order to study the temporal behavior of the source, we accumulated its PN light curve in the whole energy range 0.2–10 keV and in the two sub-ranges 0.2–2 and 2–10 keV, using an extraction radius of 30''. The corresponding background curves were extracted over the part of the CCD area not affected by the wings of the source *Point Spread Function*. The background-subtracted light curve in the whole energy range shows some variability. The light curve binned at 1000 seconds gives a reduced $\chi^2_\nu=2.6$ when fitted to a constant value and shows variations up to $\sim 30\%$ around the average level. The hardness ratio between the two sub-ranges is consistent with a constant value, indicating that no significant spectral variations took place along the observation. Therefore we performed a single spectral analysis on the whole set of data.

For the PN spectra of both the source and the background, we considered the same focal plane areas used for the light-curves. We used the *SAS* software to calculate the applicable response matrix. The accumulated source spectrum was rebinned in order to have at least 30 counts in each energy bin. For the spectral analysis we used *XSPEC* 11.2.0. The source spectrum was fitted with an absorbed power-law model, in the energy range 0.3–8.5 keV: the best-fit parameters are reported in Tab. 1. In Fig.1 we show the PN spectrum and the best-fit power-law model.

Fits with simple thermal emission models provided unacceptable results. For example, with a bremsstrahlung model we obtained $\chi^2_\nu = 1.234$, while a multi-temperature blackbody ac-

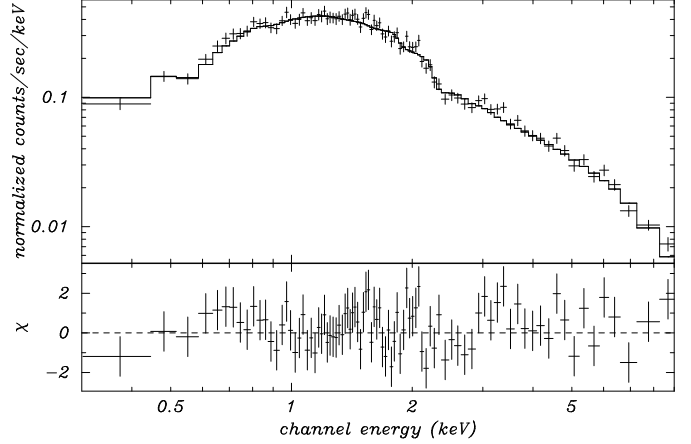


Fig. 1. Comparison of the PN spectra of 4U 1543-475 with the best-fit power-law model. In the lower panel the residuals (in units of σ) between data and model are shown.

cretion disk (*diskbb* in *XSPEC*) gave $\chi^2_\nu = 1.907$, always with 297 d.o.f.

For the MOS2 camera³ we applied the same source extraction radius of the PN camera (30''), while, thanks to the larger size of the MOS CCDs, we could accumulate the background spectrum using a circular area of 2.5' radius. Also in this case the spectrum was rebinned with a minimum of 30 counts in each energy bin and fitted over the 0.3–8.5 keV energy range. The fit with a power-law yielded a comparable photon-index but a higher hydrogen column density than the PN one (Tab. 1). This discrepancy is likely due to the uncertainties still remaining in the calibration of the two instruments, especially at low energies (Kirsch 2004). We also fitted the PN and MOS2 data simultaneously, after including a systematic error of 5% in the spectral bins. Again a satisfactory fit was obtained with a power-law model (see Table 1) while thermal models gave worse χ^2 values.

In conclusion, although the exact value of the absorption is still subject to some uncertainty⁴, all our data point to a power-law spectrum with photon index ~ 2 . In the following analysis, aimed to assess the possible presence of additional components in the spectrum, we will consider only the PN data, due to their higher statistics (~ 12000 source counts are detected in the PN

¹ the PN pixels are larger than the MOS ones; therefore, no multi-pixel events are expected by the soft-protons

² this is smaller than the MOS one due to the reduced live-time of the Small Window mode used for the PN

³ we have not used the MOS1 data since the spectral response in Timing Mode is not yet well calibrated

⁴ note, however, that this is one of the best measurements of N_H for this source obtained so far; our value is comparable with the value of $(4.26 \pm 0.15) \times 10^{21} \text{ cm}^{-2}$ obtained by van der Woerd et al. (1989) with *EXOSAT* data

Table 2. Upper limits (3σ confidence level) on the Equivalent Width of an emission line (gaussian model), at various energies and widths.

E (keV)	6	6.4	6.7	7
σ (keV)	U.L. (eV)	U.L. (eV)	U.L. (eV)	U.L. (eV)
0	173	117	37	97
0.1	209	130	48	99
0.2	255	150	71	91
0.3	262	161	90	97
0.4	254	173	113	111
0.5	235	176	138	134

compared to ~ 5600 in the MOS2). We checked that similar results would be obtained using the MOS2 data, although with looser upper limits (usually a factor 2–5 times higher).

To look for a possible Fe K_{α} emission line, we tried to improve the spectral fit by adding a gaussian component at four different fixed energies between 6 and 7 keV, with σ between 0 and 0.5 keV. In all the cases we found no evidence for it: the gaussian normalization was always consistent with zero. The upper limit on the line equivalent width is always below ~ 0.25 keV at a 3σ confidence level (Tab. 2).

Although not formally required by the data, which are satisfactorily fit by the power-law model, we investigated the possible presence of an additional multi-colour disk emission (Mitsuda et al. 1984; Makishima et al. 1986). To this aim we added a *disk blackbody* component and obtained $N_H = (4.4 \pm 0.7) \times 10^{21} \text{ cm}^{-2}$, $\Gamma = 1.94 \pm 0.05$, $K_{PL} = (1.0 \pm 0.1) \times 10^{-3}$, $kT_{col} = 0.16 \pm 0.03 \text{ keV}$ and $K_{DBB} = 141 \pm 289$ as best-fit parameters, with $\chi^2/\text{d.o.f.} = 325.5853/295$. This result would imply an absorbed flux $f_{DBB}^{0.3-10} = 8.44 \times 10^{-14} \text{ erg cm}^{-2} \text{ s}^{-1}$ for the thermal component (i.e. $\sim 2\%$ of the total flux), but the large error on its normalization clearly demonstrates that this component is only marginally present. The F-test proves that the fit quality improves only at a 0.3σ level.

We have therefore computed an upper limit to the disk emission component. This is shown in Fig. 2, where the upper-limit on the disk bolometric luminosity is shown as a function of the colour temperature T_{col} (assuming a source distance $d = 7.5 \text{ kpc}$). The power-law best-fit parameters imply an unabsorbed flux $f_X = (5.83 \pm 0.29) \times 10^{-12} \text{ erg cm}^{-2} \text{ s}^{-1}$ in the energy range 0.3–10 keV, which corresponds to $L_X = (3.92 \pm 0.20) \times 10^{34} \text{ erg s}^{-1}$. This means that any possible disk contribution is well below 10 % of the total source luminosity.

3. Discussion and conclusions

The *XMM–Newton* data reported here were obtained just two months after the start of the source outburst observed by *Ross–XTE* (*RXTE*) on MJD 52445 (2002 June 20). The source was monitored by *RXTE* during all this period: Park et al. (2004) analysed the data collected between MJD 52442 and 52477 (i.e. before the transition to the *low–hard* state), while Kalemci et al. (2004) considered the data between MJD 52464 and 52498 (i.e. during and after the transition to the *LH* state). Both Park et al. (2004) and Kalemci et al. (2004) used the sum

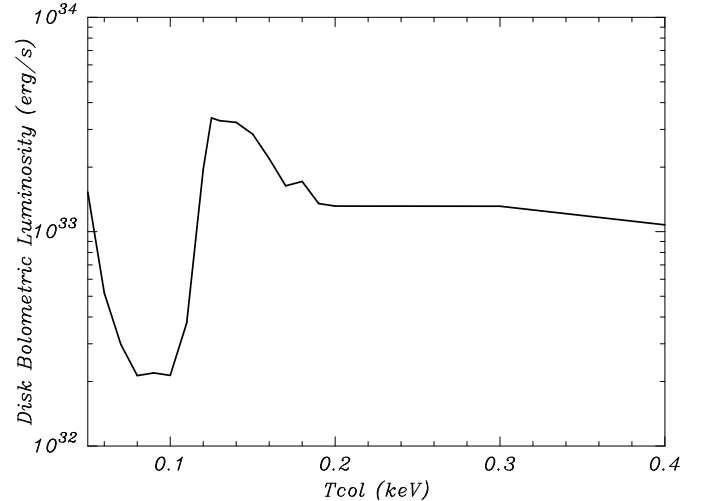


Fig. 2. 3σ upper-limit on the bolometric luminosity of the multi-colour disk as a function of the colour temperature.

of a power-law and a multi-colour disk blackbody to fit the continuum part of the spectra, finding that the photon index decreased from 3.85 (at the outburst peak) to 2.21 (just ~ 6 days before the *XMM–Newton* observation), while the temperature at the inner disk edge decreased from 1 to 0.35 keV. Using the best-fit parameters reported by these authors, we computed the 2–10 keV fluxes as a function of time for the total emission and for the power law component only, which are shown in Fig. 3. The last point in the figure indicates our *XMM–Newton* flux value, converted to the same energy range. Even if this flux is below the extrapolation of the last *RXTE* measurements, the plot shows that it is in general agreement with the overall decreasing rate measured by *RXTE*.

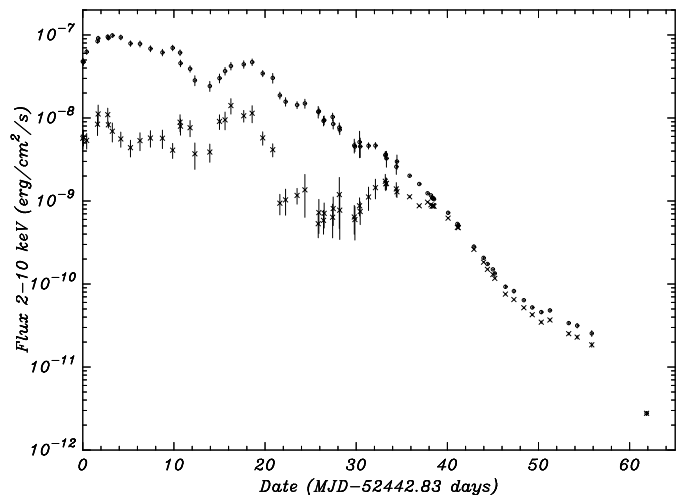


Fig. 3. X-ray flux observed by *RXTE* and *XMM–Newton* during the 2002 outburst of 4U 1543-475. The open circles refer to the total source flux, the crosses to the power-law component. The last point to the right is our *XMM–Newton* total flux

The luminosity observed with *XMM–Newton* corresponds to $\sim 1.5 \times 10^{-5}$ of the *Eddington* luminosity, still well

above the typical quiescent level of BH candidates $L_q \sim 10^{-8.5} L_{EDD}$ (Mc Clintock & Remillard 2003), where we assumed $d = 7.5$ kpc and $M = 9.4 M_\odot$. At the time of the *XMM-Newton* observation (i.e. two months after the outburst), 4U 1543-475 was not yet in quiescence but still in the low-hard state, which is characterized by $1.5 < \Gamma < 2.1$ and a power-law flux contribution higher than 80 % of the total flux.

According to Kalemci et al. (2004) some emission from an accretion disk is still required by the last *RXTE* spectra of 4U 1543-475 obtained six days before the *XMM-Newton* observation reported here. Their data cannot yield a disk temperature for such a faint and soft component. Therefore Kalemci et al. fix it at the value of 0.35 keV. Assuming $d=7.5$ kpc and $i=21^\circ$, for such a temperature our upper limit on the disk blackbody normalization corresponds to a disk colour radius of $0.08 R_g$ (where $R_g = GM/c^2$ is the BH gravitational radius). The value of r_{col} obtained from the best fitting procedure of the multi-colour disk blackbody model systematically underestimates the actual disk radius (Shimura & Takahara 1995; Merloni et al. 2000). In fact $r_{in} = \eta \times g \times f_{col}^2 \times r_{col}$, where $\eta = 0.6-0.7$ is the ratio between the inner radius and the effective radius (i.e. the radius at which the temperature of the disk peaks), $g = 0.7-0.8$ takes into account the general relativistic corrections and $f_{col} = T_{col}/T_{eff}$ is the spectral hardening factor, whose value can be about 3 for low accretion rates. If we consider the maximum value for all the parameters, from $r_{col} = 0.08 R_g$ we obtain $r_{in} \sim 0.4 R_g$. This value is incompatible with the innermost stable circular orbit around a black-hole, which is $R_{ISCO} = 6 R_g$ for a Schwarzschild BH and $R_{ISCO} = R_g$ for a Kerr BH (Shapiro & Teukolsky 1983). Note that the same would be true for lower normalizations at the same temperature. Only for disk temperatures $kT_{col} < 0.25$ keV our normalization upper limits give acceptable values for the inner disk radius. For example, for $kT_{col} = 0.2$ keV we obtain $r_{col} = 0.43 R_g$, which corresponds to $r_{in} \sim 2.2 R_g$. A similar conclusion was noted in a short report on this *XMM* observation by Miller et al. (2003), but contrary to these authors we do not find a significant improvement by the inclusion of the disk component in the fit to the spectrum of 4U 1543-475.

In conclusion the observation reported here provides one of the best quality spectra for a black hole X-ray binary accreting at a low level, but still far from the quiescent state. The featureless power law energy spectrum does not give any evidence for the presence of an accretion disk. If a disk is present, it is constrained to have a luminosity of $(2-30) \times 10^{32}$ erg s⁻¹ and a temperature smaller than 0.25 keV. This is an interesting result since little is known on the possible presence and the properties of accretion disks around black-holes at these relatively low luminosities. Even if a multi-colour disk is not strictly required in the hard state from the theoretical point of view, there are some arguments in favour of it: on one hand, most common accretion models foresee the presence of a disk with a large (i.e. $\geq 100 R_g$) inner radius (Esin et al. 1997; Mc Clintock & Remillard 2003); on the other hand, a soft X-ray excess, which can be modeled with a large and cool accretion disk, has been observed in GX 339-4 (Wilms et al. 1999) and XTE J1118+480 (Mc Clintock et al. 2001; Frontera et al.

2003), albeit at higher luminosities than that reported here for 4U 1543-475.

Acknowledgements. This work is based on observations obtained with *XMM-Newton*, an ESA science mission with instruments and contributions directly funded by ESA Member States and NASA.

References

- Chevalier, C. & Ilovaisky, S. A. 1992, *IAU Circ.*, 5520, 1
 Esin, A. A., Mc Clintock, J. E., & Narayan, R. 1997, *ApJ*, 489, 865
 Frontera, F., Amati, L., Zdziarski, A. A., et al. 2003, *ApJ*, 592, 1110
 Garcia, M. R., Mc Clintock, J. E., Narayan, R., et al. 2001, *ApJ*, 553, L47
 Harmon, B. A., Wilson, R. B., Finger, M. H., et al. 1992, *IAU Circ.*, 5504, 1
 Kalemci, E., Tomsick, J. A., Buxton, M. M., et al. 2004, *ApJ*, submitted, astro-ph/0409092
 Kirsch, M. 2004, *XMM-SOC-CAL-TN-0018 Issue 2.3*
 Kitamoto, S., Miyamoto, S., Tsunemi, H., Makishima, K., & Nakagawa, M. 1984, *PASJ*, 36, 799
 Makishima, K., Maejima, Y., Mitsuda, K., et al. 1986, *ApJ*, 308, 635
 Matilsky, T. A., Giacconi, R., Gursky, H., Kellogg, E. M., & Tananbaum, H. D. 1972, *ApJ*, 174, L53
 Mc Clintock, J. E., Haswell, C. A., Garcia, M. R., et al. 2001, *ApJ*, 555, 477
 Mc Clintock, J. E. & Remillard, R. A. 2003, 'Black Hole Binaries', Chapter 4 of 'Compact Stellar X ray Sources', eds. W.H.G. Lewin and M. van der Klis, Cambridge University Press, astro-ph/0306213
 Merloni, A., Fabian, A. C., & Ross, R. R. 2000, *MNRAS*, 313, 193
 Miller, J. M., Fabian, A. C., & Lewin, W. H. G. 2003, *The Astronomer's Telegram*, 212, 1
 Mitsuda, K., Inoue, H., Koyama, K., et al. 1984, *PASJ*, 36, 741
 Orosz, J. A. 2003, in *IAU Symposium*, 365
 Orosz, J. A., Jain, R. K., Bailyn, C. D., Mc Clintock, J. E., & Remillard, R. A. 1998, *ApJ*, 499, 375
 Park, S. Q., Miller, J. M., Mc Clintock, J. E., et al. 2004, *ApJ*, 610, 378
 Shapiro, S. L. & Teukolsky, S. A. 1983, 'Black holes, white dwarfs, and neutron stars: The physics of compact objects' (New York, Wiley-Interscience, 1983, 663 p.)
 Shimura, T. & Takahara, F. 1995, *ApJ*, 445, 780
 Strüder, L., Briel, U., Dennerl, K., et al. 2001, *A&A*, 365, L18
 Tanaka, Y. & Lewin, W. H. G. 1995, in 'X ray Binaries', ed. W. H. G. Lewin, J. van Paradijs, & E. P. J. van den Heuvel, Cambridge University Press
 Turner, M. J. L., Abbey, A., Arnaud, M., et al. 2001, *A&A*, 365, L27
 van der Woerd, H., White, N. E., & Kahn, S. M. 1989, *ApJ*, 344, 320
 van Paradijs, J. & Mc Clintock, J. E. 1995, in 'X ray Binaries', ed. W. H. G. Lewin, J. van Paradijs, & E. P. J. van den Heuvel, Cambridge University Press

Wilms, J., Nowak, M. A., Dove, J. B., Fender, R. P., & di
Matteo, T. 1999, *ApJ*, 522, 460